Journal Pre-proof

Irradiation at ultra-high (FLASH) dose rates reduces acute normal tissue toxicity in the mouse gastrointestinal system

Jia-Ling Ruan Ph.D. , Carl Lee Ph.D. , Shari Wouters M.Sc. , Iain DC Tullis Ph.D. , Mieke Verslegers Ph.D. , Mohamed Mysara Ph.D. , Chee Kin Then M.Sc. , Sean C Smart Ph.D. , Mark A Hill Ph.D. , Ruth J Muschel Ph.D. , Amato J Giaccia Ph.D. , Borivoj Vojnovic Ph.D. , Anne E Kiltie Ph.D. , Kristoffer Petersson Ph.D.

PII: S0360-3016(21)02643-2
DOI: https://doi.org/10.1016/j.ijrobp.2021.08.004
Reference: ROB 27220

To appear in: *International Journal of Radiation Oncology, Biology, Physics*

Received date: 9 April 2021
Revised date: 3 August 2021
Accepted date: 4 August 2021

Please cite this article as: Jia-Ling Ruan Ph.D. , Carl Lee Ph.D. , Shari Wouters M.Sc. , Iain DC Tullis Ph.D. , Mieke Verslegers Ph.D. , Mohamed Mysara Ph.D. , Chee Kin Then M.Sc. , Sean C Smart Ph.D. , Mark A Hill Ph.D. , Ruth J Muschel Ph.D. , Amato J Giaccia Ph.D. , Borivoj Vojnovic Ph.D. , Anne E Kiltie Ph.D. , Kristoffer Petersson Ph.D. , Irradiation at ultra-high (FLASH) dose rates reduces acute normal tissue toxicity in the mouse gastrointestinal system, *International Journal of Radiation Oncology, Biology, Physics* (2021), doi: https://doi.org/10.1016/j.ijrobp.2021.08.004

Title: Irradiation at ultra-high (FLASH) dose rates reduces acute normal tissue toxicity in the mouse gastrointestinal system

Running title: FLASH reduces acute gastrointestinal toxicity

Authors: Jia-Ling Ruan Ph.D.[1], Carl Lee Ph.D.[2], Shari Wouters M.Sc.[3,4], Iain DC Tullis Ph.D.[1], Mieke Verslegers Ph.D.[3], Mohamed Mysara Ph.D.[3], Chee Kin Then M.Sc.[1], Sean C Smart Ph.D.[1], Mark A Hill Ph.D.[1], Ruth J Muschel Ph.D.[1], Amato J Giaccia Ph.D.[1], Borivoj Vojnovic Ph.D.[1], Anne E Kiltie Ph.D.[1]*, Kristoffer Petersson Ph.D.[1,5]*

[1]MRC Oxford Institute for Radiation Oncology, Department of Oncology, University of Oxford, Old Road Campus Research Building, Roosevelt Drive, Oxford OX3 7DQ
[2]Kennedy Institute of Rheumatology, Nuffield Department of Orthopaedics, Rheumatology and Musculoskeletal Science, University of Oxford, Oxford, United Kingdom
[3]Interdisciplinary Biosciences Group, Belgian Nuclear Research Centre (SCK CEN), Mol, Belgium
[4]Molecular pathology group, Cell Biology and Histology and Laboratory of Medical Microbiology, Vaccine & Infectious Disease Institute, Campus Drie Eiken, University of Antwerp, Antwerp, Belgium
[5]Radiation Physics, Department of Haematology, Oncology and Radiation Physics, Skåne University Hospital, Lund, Sweden
* Equal contribution
Corresponding Author: Kristoffer Petersson Ph.D., Department of Oncology, University of Oxford, Off Roosevelt Drive, Oxford OX3 7DQ, United Kingdom. Phone: +44 1865 617416; E-mail: kristoffer.petersson@oncology.ox.ac.uk

Author responsible for statistical analysis: Jia-Ling Ruan Ph.D., E-mail: jia-ling.ruan@oncology.ox.ac.uk
Conflict of Interest: None

Funding Statement: This study was funded by Cancer Research UK – RadNet Grant (C6078/A28736) and the Medical Research Council – MRC (MC_UU_00001/9). Shari Wouters PhD studentship was funded by SCK CEN.

Data Availability Statement for this Work: Research data are stored in an institutional repository and will be shared upon request by the corresponding author. The microbiome data has been deposited into the NCBI Sequence Read Archive (Study PRJNA705831) (ftp://ftp-trace.ncbi.nlm.nih.gov/sra/review/SRP308778_20210303_122254_791d77ef3e56755b30135cc31166f5a8) to be made public on publication.

Acknowledgements: This study was funded by Cancer Research UK – RadNet Grant (C6078/A28736) and the Medical Research Council – MRC (MC_UU_00001/9). Shari Wouters PhD studentship was funded by SCK CEN. We thank the staff of the Oncology mechanical workshop, Mr J Prentice, Mr G Shortland and Mr K Hallett, for fabrication of various components used for the animal setup. We also thank Ms Karla Watson and Magdalena Hutchins of the Oncology Biomedical Science Unit for assistance with animal maintenance.

Abstract (286 words)

Purpose:

Preclinical studies using ultra-high dose rate (FLASH) irradiation have demonstrated reduced normal tissue toxicity compared to conventional dose rate (CONV) irradiation, although this finding is not universal. We investigated the effect of temporal pulse structure and average dose rate of FLASH compared to CONV irradiation, on acute intestinal toxicity.

Materials and Methods:

Whole abdomens of C3H mice were irradiated with a single fraction to various doses, using a 6 MeV electron linear accelerator (LINAC), with single pulse FLASH (dose rate =2-6$\times 10^6$ Gy/s) or conventional (CONV; 0.25 Gy/s) irradiation. At 3.75 days post-irradiation, fresh feces were collected for 16S rRNA sequencing to assess changes in the gut microbiota. A Swiss roll-based crypt assay was used to quantify acute damage to the intestinal crypts to determine how tissue toxicity was affected by the different temporal pulse structures of FLASH delivery.

Results:

We found statistically significant improvements in crypt survival for mice irradiated with FLASH at doses between 7.5 and 12.5 Gy, with a dose modifying factor of 1.1 for FLASH (7.5 Gy, $p < 0.01$; 10 Gy, $p < 0.05$; 12.5 Gy, $p < 0.01$). This sparing effect was lost when the delivery time was increased, either by

increasing the number of irradiation pulses or by prolonging the time between two successive pulses. Sparing was observed for average dose rates of ≥280 Gy/s. Fecal microbiome analysis showed that FLASH irradiation caused fewer changes to the microbiota than CONV irradiation.

Conclusions:

This study demonstrates that FLASH irradiation can spare mouse small intestinal crypts and reduce changes in gut microbiome composition compared to CONV irradiation. The higher the average dose rate, the larger the FLASH effect, which is also influenced by temporal pulse structure of the delivery.

Introduction

More than half of all cancer patients receive radiotherapy, in curative or palliative settings (1). However, treatment efficacy of cancer radiotherapy is generally limited by radiation-induced normal tissue toxicities. Recently FLASH radiotherapy has been shown to reduce normal tissue toxicity while maintaining the cancer therapeutic efficacy seen with conventional dose rate (CONV) radiotherapy in some preclinical and clinical studies (2). FLASH radiotherapy generally involves irradiation (IR) delivered at ultra-high dose rate (average dose rate ≥ 40 Gy/s) in contrast to CONV radiotherapy (2-20 Gy/min), resulting in significantly reduced treatment times from several minutes to just fractions of a second. However, not all FLASH IR studies have shown increased normal tissue sparing. Smyth *et al.* found no change in median toxic dose for mice following total or partial body IR, at an ultra-high dose rate of 37-41 Gy/s compared to a conventional dose rate of a few Gy/min (3). Venkatesulu *et al.* reported increased toxicity of murine immune system and gastrointestinal toxicity in mice receiving 35 Gy/s FLASH whole abdominal IR (4). In contrast, improved survival for mice following partial body IR at ultra-high dose rate (70-210 Gy/s) was demonstrated by other groups (5). Using a murine brain cognition model, Montay-Gruel *et al.* showed that dose rate is crucial for the FLASH neuroprotective effect; sparing of memory was seen at dose rates ≥ 30 Gy/s, with increasing sparing as the dose rate increased to ≥ 100 Gy/s (6). A subsequent study showed a large FLASH sparing effect in irradiated pig skin, as well

as good therapeutic results in the first veterinarian clinical FLASH study, treating feline patients (7). Recently, single fraction FLASH radiotherapy was shown to produce great therapeutic results with limited toxicity for the treatment of tumors, such as squamous cell carcinoma and soft tissue sarcoma, in canine cancer patients (8). Studies have also shown improvement in survival and development of zebrafish embryos irradiated with FLASH (10^6-10^7 Gy/s) compared to CONV IR (9,10). Pawelke J *et al.* showed a similar benefit following zebrafish IR using an electron FLASH beam at 10^5 Gy/s (11), while a previous study by the same group showed that proton FLASH IR at a dose rate of 100 Gy/s had no improvement in survival and development compared to CONV IR (12). The discrepancies between current published studies suggest that further investigations are required into the optimal conditions for inducing the protective FLASH effect.

Radiation-induced gastrointestinal (GI) toxicity is the major dose-limiting factor in treating many pelvic or abdominal cancers, with 60-80% of these patients developing symptoms of acute GI toxicity during radiotherapy (13). The toxicity results primarily from the death of rapidly proliferating stem cells in the crypts, subsequently leading to insufficient replacement of the intestinal epithelium, mucosal barrier disruption, bacterial translocation and inflammation. Disruption of the intestinal crypts has been used as a quantitative assay to study radiation-induced intestinal damage since 1970 (14).

As well as directly damaging the intestinal tissue, radiation exerts GI toxicity by inducing a substantial shift in gut microbial composition (15,16). In turn, this can lead to epithelial destruction and inflammation (17), thus exacerbating initial tissue damage. Consequently, patients may experience diarrhea, fatigue, rectal bleeding and malabsorption. These might require additional treatment or even premature treatment cessation (18,19). Further to the possible negative effects on the treatment plan and the care cost, the negative effect on patient quality of life is also important to consider. Recent studies on the gut microbiome showed that it can modulate the therapeutic response of cancers (20).

Melanoma patients who responded well to PD-1 checkpoint blockade immunotherapy showed higher microbiome diversity and more abundance of commensal microbiome species (21,22). Therefore, insight into the microbiome dynamics post-IR and how this might differ for FLASH IR compared to CONV IR is important.

In this study, we conducted single dose whole abdominal IR on C3H mice with either FLASH or CONV IR, delivered by an in-house developed electron linear accelerator (LINAC) and systematically quantified acute GI toxicity using a Swiss roll-based crypt assay. Additionally, alterations to gut microbiota composition were assessed by 16S rRNA sequencing of fecal samples. We further investigated the effect on intestinal tissue toxicity by radiation dose rate, number of pulses, and the pulse interval for the FLASH IR.

Material and Methods

All experiments were carried out on our FLASH-optimized in-house developed LINAC, delivering electrons of 6 MeV nominal energy with a circular horizontal beam of 5 cm in diameter, which has been described in more detail elsewhere (23). All animal research was conducted in accordance with United Kingdom Home Office Guidelines and institutional guidelines, under XXXX project licenses XXXX and XXXX.

Whole-abdominal irradiation with FLASH and conventional dose rate

Female C3H mice (145 mice aged 9-10 weeks old, average weight: 23.02 $\pm$ 0.15 g and 90 mice aged 30-31 weeks old, average weight of 40.84 $\pm$ 0.50 g, all from Charles River) were used. Mice were acclimatized before starting the experiment. Six mice were housed per individually ventilated cage in a 12/12-hour light/dark cycle. Mice were fed with regular chow and provided with drinking water *ad libitum*. Mice were randomly assigned to different treatment or sham control groups (non-anaesthetized, non-irradiated). All Conv IR and FLASH IR mice were anesthetized using isoflurane supplemented with

95% oxygen (4% for anesthetic induction and 2% for maintenance, total anaesthesia time < 10 min) and then placed in a mouse cradle based upon the designs described elsewhere (24) in front of the horizontal radiation beam (Figure 1). The mouse was irradiated at room temperature, in an upright position (Figure 1) with a 33 x 30 cm^2 (height x width) radiation field (collimated by a 6 mm thick brass plate just upstream of the mouse) covering the whole abdomen, with FLASH or CONV IR. CONV IR consisted of multiple (≈ 750-1,500) electron pulses, delivered at a pulse repetition rate of 25 Hz and at an average dose rate of 15 Gy/min (= 0.25 Gy/s, dose-per-pulse ≈ 10 mGy, pulse dose rate ≈ 3×10^3 Gy/s). When compared to CONV IR, the FLASH delivery consisted of a single 3.4 µs wide electron (macro)pulse delivering doses ranging from 7.5 to 20 Gy by adjusting the scattering foil (a titanium foil, 30 µm thick, positioned 8.5 mm downstream from the beamline exit window) to-collimator distance (35-57 cm for FLASH, 45 cm used for CONV), i.e. with average (and pulse) dose rates of 2.2-5.9 $\times$ 10^6 Gy/s depending on the delivered dose.

The importance of the temporal pulse structure for the FLASH effect

For this investigation, 11.2 Gy and 12.5 Gy were delivered in 9-10- and 30-31-weeks old mice, respectively. The number of pulses of the dose delivery was varied (from 1-300 and 1-1250, for 11.2 Gy and 12.5 Gy deliveries, respectively), requiring correspondingly lower dose-per-pulse and dose rate values and longer delivery times for consistent dose delivery, which was achieved by lowering the electron gun current. Furthermore, a dual-pulse delivery (of equal dose-per-pulse) was also performed with varying time between the two pulses (pulse intervals, from 3.3 ms -30 s).

Dosimetry

The dosimetry was verified before and after each mouse IR with Gafchromic EBT-XD film (Ashland Inc., Covington, KY, USA), positioned in-between two Perspex pieces of a mice phantom which was positioned exactly as the mice in the beam path (Supplementary Figures 1 and 2). The films were

read 24 h post-IR with a film scanner (Epson Perfection v850 Pro, Seiko Epson Corporation, Nagano, Japan) and the red channel analyzed with ImageJ (version 1.52a, Wayne Rasband, NIH, USA). The dose was averaged over a 20 x 20 mm^2 central part of the exposed part of the film. The films had previously been calibrated in a 6 MeV clinical electron beam from a Varian Truebeam (Varian Medical Systems Inc., Palo Alto, CA, USA) linear accelerator, at the XXXX (25). For on-line verification of the dose delivery, a toroidal beam charge monitor (XXXX) as well as a beam energy monitor was used, described in (23). The energy monitor was also used to verify that the electron beam energy was consistently 6 MeV. Our overall uncertainty in dosimetry is estimated to be 4% (including a measured output variation of our FLASH and CONV IR deliveries of within 2%).

CONV IR was performed by decreasing the pulse rate and by reducing the peak pulse current. The pulse current reduction would normally increase spectral fluence (23) to >8 MeV due to reduced beam loading mechanisms. However, we maintained the spectral fluence at the same levels as that used for FLASH IR by reducing the radiofrequency power fed to the accelerator waveguide through slight (≈200 kHz) detuning of the radiofrequency source from its nominal 2.998 GHz. The consequences of this detuning were verified with percentage depth dose measurement using film in a solid water phantom (Supplementary Figure 3) and verified on-line for every delivery with our beam energy monitor.

Swiss roll-based crypt assay to quantify intestine toxicity

Following IR, the mice were monitored and weighed daily. Mice were killed 3.75 days post-IR. The intestines were collected, processed, and analyzed as described previously (26). In brief, the small intestine was flushed with PBS to remove feces and then equally divided into three segments. Micro-scissors were used to open the lumen of each segment and the colon. Once the lumen was opened, sharp tweezers were used to roll the intestine from the posterior end, with the inner lumen now facing outward. The tissues were then fixed with 10% neutral buffer formalin overnight and stored in 70%

ethanol for paraffin embedding. Five micrometer sections were cut and stained for hematoxylin and eosin (H&E).

A modified Swiss roll-based crypt assay as described in (26) was used to quantify the acute crypt damage caused by ionizing radiation. Briefly, H&E-stained slides were anonymized and scanned using an Aperio CS2 digital pathology scanner (Leica Camera AG, Wetzlar, Germany) and images were examined using the Aperio ImageScope Viewer software (Leica Camera AG). From each segment, the most severely damaged part, as defined by > 3 mm region with least number of crypts, was chosen from two independent assessments and the consensus was reached before further counting. The number of crypts from the whole > 3 mm region was counted from each part. Only the crypts with > 10 cells and showing no sign of apoptosis were counted as regenerating crypts. For each experimental group, age-matched non-irradiated mice were used as the control. The percentage of remaining crypts (% crypts remaining) was used as an indicator of crypt survival and calculated as:

$$\frac{number\ of\ regenerating\ crypts\ per\ mm}{number\ of\ control\ crypts\ per\ mm} \text{ x } 100$$

Statistical analysis was performed using Graph Pad Prism software (GraphPad Software Inc., La Jolla, CA, USA). All values are presented as mean ± standard error of mean (SEM). The number of animals used as biologically independent replicates is indicated by *n*. Data were checked for normality and equal variance. For normally distributed data with equal variance, Student's t-test was used to compare the difference between two groups, while one-way analysis of variance (ANOVA) was used to compare the difference between multiple groups with *post hoc* Tukey multiple comparison. For data failing to pass normality or equal variance test, non-parametric tests (Mann-Whitney U test for two groups and Kruskal-Wallis test with Dunn's multiple comparison test for multiple groups) were performed. The crypt survival results were fitted with a sigmoidal dose response model (Nonlinear regression analysis) in Prism software.

Microbial analysis following FLASH and conventional dose rate irradiation

For microbial analysis, fresh feces were collected within a 30-minute time range before the mice were killed, from C3H mice (9 weeks old, total 17 mice) including controls (*n* = 6) and those irradiated using FLASH or CONV IR to 12.5 Gy (*n* = 6 for FLASH IR, *n* = 5 for CONV IR, as one mouse did not produce feces at the time point). Feces were snap frozen on dry ice and stored at -80 ^{o}C. DNA was extracted using the DNeasy PowerSoil Pro Kit (Qiagen, 47016, The Netherlands) according to the manufacturer's instructions. Extracted dsDNA was quantified using the QuantiFluor® dsDNA System kit (Promega Corporation, E2670, The Netherlands) and was sent for V3-V4 16S rRNA sequencing to BaseClear (Leiden, The Netherlands). Sequencing data were deposited in the NCBI Sequence Read Archive (Study PRJNA705831). A positive control (cell mock sample, ZymoBIOMICS^{TM}, D6331) and a negative control (blank sample) were included. Sequencing data was analyzed through the OCToPUS pipeline (27) resulting in operational taxonomic units (OTUs) with a clustering cut-off of 97%. The alignment and classification were performed against the SILVA database (v119), using the Ribosomal Database Project (RDP) dataset (v.16) (classification cut-

off of 80%). For the α- and β-diversity analysis, total counts of each samples were subsampled to the smallest sampling depth among them, so more sequences per sample were retained.

The α-diversity indices were calculated using Chao, Simpson evenness and inverse Simpson for richness, evenness and overall diversity (*single.summary* command in mothur, an open-source software package for bioinformatics data processing), respectively. The β-diversity was estimated through UniFrac analysis based on weighted metric (using *dist.shared* command in mothur) and visualized using principal coordinate analysis (PCoA, using *pcoa* command in mothur). For statistical comparison of α-diversity, Shapiro and Bartlett tests were used to assess the normality and homoscedasticity, respectively. Whenever normality and homoscedasticity were met, an ANOVA test (followed by a Student's t-test) were used, otherwise a non-parametric Kruskal-Wallis test (followed by Mann-Whitney U test) was applied. Bonferroni correction was applied for test p-values. For β-diversity, analysis of molecular variance (AMOVA, i.e. an ANOVA-like statistical method) was used to compare the diversity between samples (using the mothur *amova* command).

The identification of significant differences in the relative abundance of OTUs was conducted using Linear Discriminant Analysis (LDA) Effect Size (LEfSe)(28). Only OTUs with LDA > 3 at a p value < 0.05 were considered differentially abundant. Functional predictions were conducted using PICRUSt (v.1.1.2) based on the Kyoto Encyclopedia of Genes and Genomes (KEGG) database (29). Statistical comparison between conditions was conducted in STAMP (v.2.1.3) (30). The predicted pathways were compared using Welch's t-testing (p-values were corrected using false discovery rate) and filtered using an effect size ratio of 2. Correlations between microbial data and metadata were calculated using Spearman's rank correlation coefficient, ρ. Correlations were identified as strong for $\rho > |0.7|$. Statistical analysis was performed using Student's t-test.

Results

Ultra-high dose rate FLASH IR spares acute intestinal toxicity

For the crypt assay, the most damaged intestinal section in irradiated mice was generally found in segments 2 (jejunum) and 3 (ileum). In those segments, control mice had 16.6 ± 0.6 crypts/mm and 16.3 ± 0.6 crypts/mm, respectively. The number of crypts in the damaged area was normalized to the crypt numbers from non-irradiated control mice to show the remaining crypt percentage as an indicator of crypt survival. A statistically significant difference in the remaining crypts was observed when comparing mice irradiated with CONV and FLASH IR within 7.5 to 12.5 Gy (Figure 2A, 7.5 Gy, $p < 0.01$; 10 Gy, $p < 0.05$; 12.5 Gy, $p < 0.01$, $n = 6$ for each group). Based on the nonlinear regression analysis, the dose to achieve 10% remaining crypts for the CONV IR was 12.7 Gy (CI: 12.1 to 13.4 Gy, $R^2 = 0.98$) and for the FLASH IR was 13.9 Gy (CI: 13.3 to 14.7 Gy, $R^2 = 0.99$), which results in a dose modifying factor of 1.1. We also irradiated the 30-31 weeks old mice with both CONV and FLASH IR from 5 to 12.5 Gy and found a significant difference in the remaining crypts at 12.5 Gy (Figure 2B, $p < 0.01$, $n = 4$ for 0 Gy and 12.5 Gy FLASH IR, $n = 6$ for 5 Gy, $n = 3$ for 10 Gy) and a dose modifying factor of 1.1 ($R^2 = 0.98$ for both CONV and FLASH IR groups).

The weight loss of mice at the 3.75-day post-IR endpoint showed a small but not statistically significant difference for mice receiving ultra-high dose rate FLASH IR compared to CONV IR (Supplementary Figure 4 and Supplementary Tables 1 and 2), although an overall radiation-induced decrease in body weight irrespective of the IR protocol could be demonstrated ($p < 0.001$).

Ultra-high dose rate FLASH IR caused less alteration of the gut microbiota

Microbiome analysis (Figure 3, $n = 5$ for CONV IR, $n = 6$ for FLASH IR and CTRL) was conducted on fresh fecal samples from non-irradiated mice (CTRL) as well as mice irradiated with ≈12.5 Gy CONV IR (measured by film to be 12.8 Gy, ≈1250 pulses at an average dose rate of 15 Gy/min) or FLASH IR (measured by film to be 12.4 Gy, single pulse, at a dose rate of 3.5×10^6 Gy/s). Relative abundance of OTUs for each sample was shown in Figure 3A.

Microbial α-diversity was assessed using three indices: overall α-diversity (i.e. diversity within a sample, considering both richness and evenness, shown by inverse Simpson index), evenness (the percentage of each bacterial taxa and how evenly these are distributed within a single sample, shown by Simpson evenness index) and richness (number of detected bacterial taxa, shown by Chao index). A drop in overall α-diversity and evenness was observed in both IR groups when compared to CTRL while no difference was detected when comparing CONV IR to FLASH IR (Figure 3, CTRL vs. CONV IR, $p < 0.05$; CTRL vs. FLASH IR, $p < 0.01$; CTRL vs. CONV IR, $p < 0.01$; CTRL vs. FLASH IR, $p < 0.001$ respectively for overall diversity and evenness).

In contrast, the richness was only lower in CONV IR mice, but not in FLASH IR mice, when compared to non-irradiated CTRL mice. Moreover, a significant difference was detected between CONV IR and FLASH IR mice (Figure 3D, CONV IR vs. CTRL and CONV IR vs. FLASH IR, $p < 0.001$). To identify potential correlations between radiation-induced microbial changes, intestinal toxicity and other clinical parameters, Spearman correlations were assessed including data of both IR groups and the CTRL group. Positive correlations were identified for overall α-diversity when compared to body weight change ($\rho = 0.650$, $p < 0.01$) and remaining crypts ($\rho = 0.753$, $p < 0.001$) (Supplementary Figure 5).

Distinct microbiome clusters were detected by β-diversity analysis (i.e. diversity between samples without the consideration of abundances) for CTRL, CONV IR, and FLASH IR groups (Figure 3E, CTRL vs. CONV IR, $p = 0.001$; CTRL vs. FLASH IR, $p = 0.002$; CONV IR vs. FLASH IR, $p < 0.001$). The FLASH IR cluster was closer to the CTRL cluster, indicating less alteration of the microbiome compared to the CONV IR group.

Post-IR, LEfSe analyzes showed a more prominent distinction between CTRL and CONV IR as compared to CTRL and FLASH IR (Figure 3F, Supplementary Table 3). In particular, it revealed an overall decrease in *Clostridia*, *Bacteroidetes*, *Actinobacteria* and *Tenericutes* taxa and an overall increase in *Bacilli*, *Deferribacteres*, *Verrucomicrobia* and *Proteobacteria* taxa in CONV IR as compared to CTRL. Species

enriched after CONV IR, including *Enterococcus spp. and Parabacteroides spp.* were negatively correlated with percentage of remaining crypts which was not observed for species enriched after FLASH IR.

Microbiome-based functional prediction revealed differences between CONV and FLASH IR, including an increase in bacterial invasion of epithelial cells, bile secretion and arachidonic acid metabolism in CONV IR as compared to FLASH IR (Supplementary Figure 6).

Increasing number of pulses or the time between two pulses decreased crypt survival

We sought to test the effect of different temporal pulse structures on the FLASH effect. Mice were subject to 11.2 Gy whole abdominal IR with different numbers of pulses. An increase in the number of pulses (with a corresponding decrease in dose-per-pulse, pulse and average dose rates, and an increase in delivery time) from single pulse to multiple pulses significantly decreased crypt survival (Figure 4A, Table 1, n = 3 for 300 pulses and n = 4 for the other groups). The single pulse group showed 27.6 ± 4.0% remaining crypts, while delivering 2, 5, and 30 pulses approximately halved crypt survival. Delivering 100 and 300 pulses further reduced crypt survival (Figure 4 A, Table 1).

A significant difference in crypt survival (about half the value) was also found between single pulse and a dual-pulse delivery with pulse intervals of 0.003 and 0.01 s, while further prolonging the pulse interval resulted in another reduction (again about half the values) in the remaining crypts (Figure 4B, Table 1, n = 3 for 30 sec and n = 4 for the other groups).

A similar trend of crypt reduction was found for mice irradiated with 12.5 Gy with a dual-pulse delivery with different pulse intervals (Supplementary Figure 7). Converting both datasets into the total delivery time, we showed that increasing the total delivery time, i.e. reducing the average dose rate, resulted in less crypt survival (Figure 4C). At the same total delivery time of 0.04 s (and average dose rate of 280 Gy/s), delivering 11.2 Gy using 5 pulses showed a higher crypt survival than using two pulses at 0.04 s

interval ($p = 0.05$). Overall, while a difference in crypt survival was seen for different radiation parameters, no difference was found between groups for weight loss at 3.75 days.

Experiments were also performed using older mice (30-31 weeks), which weighed about twice as much as the 9-week-old mice ($p < 0.0001$). Delivering 12.5 Gy whole abdominal IR with just 1 and 2 pulses resulted in 11.0 ± 2.8% and 16.4 ± 5.8% remaining crypts, which are significantly higher compared to groups of mice irradiated with CONV IR using 1250 pulses (Figure 4D, Table 2, $n = 4$ for 1, 100, and 300 pulses, $n = 3$ for 1250 pulses and $n = 5$ for the other groups). Higher remaining crypts were also found for 12.5 Gy with a dual-pulse delivery with pulse intervals of 0.003, 0.01 and 0.04 s compared to 3 and 30 s pulse intervals (Figure 4E, Table 2, $n = 4$ for 0.003 s and $n = 5$ for the other groups), though statistical significance was only found between 0.04 s and 3 s ($p < 0.05$). When converting both datasets into the total delivery time (and average dose rate), we again showed that increasing the total delivery time, and reducing the average dose rate, resulted in reduced crypt survival (Figure 4F, Table 2). In these older mice, at the total delivery time of 0.04 s (and average dose rate of 310 Gy/s), delivering 12.5 Gy using 5 pulses showed a trend for reduction in crypt survival compared to using two pulses ($p = 0.06$). As for the 9-10 weeks old mice, no significant difference was found between groups for weight loss at 3.75 days.

Discussion

In this study, we revealed a FLASH sparing effect for acute gastrointestinal toxicity, with a dose modifying factor of 1.1 at 7.5-12.5 Gy IR dose as well as a 2-3-fold increase in the remaining crypts at 11.2 and 12.5 Gy IR dose (albeit for a low level of remaining crypts at these relatively toxic doses), between ultra-high dose rate FLASH and CONV IR, assessed by crypt survival in mice at 3.75 days following whole abdominal IR. Previous normal tissue sparing studies by ultra-high dose rate FLASH IR have reported either dose modifying factors from 1.1 to 1.8 on different IR target tissues or no observed

sparing (2). The FLASH effect has been established in skin, brain, and lung with dose modifying factors of 1.2 to 1.8, for electron, proton, and photon beams (7,9,31-36). Recently, Cunningham *et al*. confirmed a FLASH normal sparing effect (at a 115 Gy/s) in mice irradiated with proton pencil beam scanning, a technique that is now being used in clinical studies (37). The reported FLASH effect following whole abdominal IR in mice has been less marked compared to these models. Data from Loo *et al.* showed a dose modifying factor of 1.1-1.2 in lethal dose 50 (LD50) using a dose rate of 70-210 Gy/s (5). However, we used a much higher dose rate (2-6 $\times$ 10^6 Gy/s) to reach this dose modifying factor. Whole abdominal proton IR with around 100 Gy/s has also been reported as showing a significant FLASH sparing effect (38,39). In our study, average dose rates of 280 Gy/s, or higher, were needed for a significant FLASH effect on crypt survival. Furthermore, we showed that a single pulse of IR, i.e. at the highest dose rate, achieved the best crypt preservation and that the normal tissue sparing effect was gradually reduced with lower averaged dose rate, which again is similar to what was reported by Loo *et al.* (5).

Additionally, we investigated the effects of FLASH IR and CONV IR on the gut microbiota. In accordance with literature (40,41), we observed a reduction in overall bacterial diversity post-IR for both FLASH and CONV IR when compared to the control group. Furthermore, a positive correlation was identified between the overall bacterial diversity and body weight change, indicating that a decreased gut diversity is linked with weight loss, irrespectively of the type of IR, which is in accordance with other preclinical studies (41). Additionally, a positive correlation between the overall bacterial diversity and the percentage of remaining crypts was found, indicating that radiation-induced alteration of the gut microbiota is linked with increased intestinal injury and thus confirming what has been described previously by Gerassy-Vainberg *et al. (17)*. Hence, the validity of our model is confirmed.

Even though no difference was observed between CONV and FLASH IR for overall bacterial diversity, CONV IR, unlike FLASH IR, resulted in a reduction in the bacterial species count post-IR and

demonstrated more change in microbiota (α- and β-diversity, Figure 3) when compared to non-irradiated control mice. This could suggest that the gut microbiome is more sensitive to CONV IR as compared to FLASH IR and was characterized by an increase in the members of the *Bacilli* class and decrease in members of the *Clostridia* class, which has previously been linked to IR-induced diarrhea in patients (42). These results suggest that the gut microbiota of CONV IR mice experience more marked changes (15,40,43).

Specifically, we identified several bacterial species that were enriched in the CONV IR group and that were negatively correlated with percentage remaining crypts, including *Enterococcus spp.* and *Parabacteroides spp.* The negative correlation suggests an association between the enrichment of a bacterial taxon and increased acute IR-induced intestinal injury. An increase in *Akkermansia spp.* and *Parabacteroides spp.* has previously been reported following radiation injury and has been correlated to radiation-induced proctitis (44). Also, the increased abundance of *Enterococcus spp.* after IR has been suggested to be associated with acute IR-induced enteritis (44). Finally, *Blautia spp.* has also been described to be increased after IR but has not yet been linked to IR-induced acute toxicity (44). In all, this suggests that acute intestinal enteritis is associated with an interplay of bacterial taxa rather than a single taxon. While such associations are generally expected following radiation exposure and reflects acute IR-induced intestinal injury, such a link was not observed following FLASH IR. Similarly, functional analysis suggested distinct microbial pathway profiles when comparing CONV and FLASH IR. In particular, an increased bacterial invasion of epithelial cells and arachidonic acid metabolism (an indicator of inflammation) was shown (Supplementary Figure 6), indicating higher intestinal injury following CONV IR (45,46). To our knowledge, we are the first to describe the microbial dynamics post-IR with ultra-high dose rate and its capacity to reduce the damage to the gut microbiome.

Some confounding factors have been identified in our microbiome analysis results. Firstly, due to animal welfare issues, the mice from the same experimental group were caged together before fecal collection from each mouse. This may result in reduction in intra-group variation. Secondly, unlike the irradiated group, the non-irradiated control group did not receive anesthesia, which might contribute to inflating the microbial distance from the irradiated group (47). Yet, this provides more insight on the differential dysbiosis of the two irradiation methods compared to the healthy, non-disturbed control community, which is the main objective of our study. Lastly, the difference in the fecal collection times of the day may affect these results, although we found no correlation between the collection time and the microbial shift.

Our study further investigated the importance of the temporal pulse structure of the delivery and its consequences for the FLASH effect. Some of our delivery parameters are similar to Levy *et al.* (48) who showed a FLASH effect after whole abdominal IR. They demonstrated that 7-8 pulses of ultra-high dose rate IR (2 Gy/pulse, averaged dose rate 216 Gy/s, 9 ms pulse interval) resulted in a ≈2.5 fold increase in preserved regenerating crypts (48). In our study, a similar averaged dose rate (280 Gy/s) also showed a 2 to 3-fold increase in crypt survival in mice, as compared to groups of mice exposed to lower dose rates, although a higher crypt preservation was found with a single pulse IR. Venkatesulu *et al.* showed that instead of sparing normal tissue, 35 Gy/s ultra-high dose rate IR caused more acute gastrointestinal toxicity in mice compared to CONV IR (4). The reason for this might have been differences in setup and energy spectrum between FLASH and CONV in their study, resulting in differences in dose distributions in the mice. In our study, a similar dose rate (39 Gy/s) showed a slight (non-significant) normal tissue sparing effect.

Conclusion

In this study, we investigated the FLASH effect on acute intestinal toxicity following whole abdominal IR of mice. The normal tissue toxicity was systematically quantified by a modified Swiss roll-based crypt assay. A 10% reduction in normal tissue toxicity was observed when the dose was delivered in a single 3.4 μs pulse compared to IR at a conventional dose rate (i.e. a dose modifying factor of 1.1). Increasing the number of pulses or the time interval between a dual-pulse delivery gradually increased the normal tissue toxicity, and hence decreased the FLASH effect. In addition, we showed that ultra-high dose rate FLASH IR caused less alteration of the gut microbiota compared to CONV IR, which was shown to be correlated with a reduced intestinal injury. Overall, our results confirmed the normal tissue sparing effect of ultra-high (FLASH) dose rate IR, which was correlated with the averaged dose rate, but which was also affected by the temporal pulse structure of the IR delivery.

References

1. Jaffray DA, Gospodarowicz MK. Radiation therapy for cancerWashington DC: The International Bank for Reconstruction and Development / The World Bank; 2015.

2. Wilson JD, Hammond EM, Higgins GS, et al. Ultra-high dose rate (flash) radiotherapy: Silver bullet or fool's gold? *Front Oncol* 2019;9:1563.

3. Smyth LML, Donoghue JF, Ventura JA, et al. Comparative toxicity of synchrotron and conventional radiation therapy based on total and partial body irradiation in a murine model. *Sci Rep* 2018;8:12044.

4. Venkatesulu BP, Sharma A, Pollard-Larkin JM, et al. Ultra high dose rate (35 gy/sec) radiation does not spare the normal tissue in cardiac and splenic models of lymphopenia and gastrointestinal syndrome. *Sci Rep* 2019;9:17180.

5. Loo BW. (p003) delivery of ultra-rapid flash radiation therapy and demonstration of normal tissue sparing after abdominal irradiation of mice - international journal of radiation oncology • biology • physics. *International Journal of Radiation Oncology Biolody Physics* 2017;98:E16.

6. XXXX

7. XXXX

8. Konradsson E, Arendt ML, Bastholm Jensen K, et al. Establishment and initial experience of clinical flash radiotherapy in canine cancer patients. *Frontiers in Oncology* 2021;11.

9. Bourhis J, Montay-Gruel P, Goncalves Jorge P, et al. Clinical translation of flash radiotherapy: Why and how? *Radiother Oncol* 2019;139:11-17.

10. Vozenin MC, Hendry JH, Limoli CL. Biological benefits of ultra-high dose rate flash radiotherapy: Sleeping beauty awoken. *Clin Oncol (R Coll Radiol)* 2019;31:407-415.

11. Pawelke J, Brand M, Hans S, et al. Electron dose rate and oxygen depletion protect zebrafish embryos from radiation damage. *Radiotherapy and Oncology* 2021.

12. Beyreuther E, Brand M, Hans S, et al. Feasibility of proton flash effect tested by zebrafish embryo irradiation. *Radiother Oncol* 2019;139:46-50.

13. Hauer-Jensen M, Denham JW, Andreyev HJN. Radiation enteropathy – pathogenesis, treatment, and prevention. *Nat Rev Gastroenterol Hepatol* 2014;11:470-9.

14. Withers HR, Elkind MM. Microcolony survival assay for cells of mouse intestinal mucosa exposed to radiation. *Int J Radiat Biol Relat Stud Phys Chem Med* 1970;17:261-7.

15. Nam YD, Kim HJ, Seo JG, et al. Impact of pelvic radiotherapy on gut microbiota of gynecological cancer patients revealed by massive pyrosequencing. *PLoS One* 2013;8:e82659.

16. Tonneau M, Elkrief A, Pasquier D, et al. The role of the gut microbiome on radiation therapy efficacy and gastrointestinal complications: A systematic review. *Radiother Oncol* 2020;156:1-9.

17. Gerassy-Vainberg S, Blatt A, Danin-Poleg Y, et al. Radiation induces proinflammatory dysbiosis: Transmission of inflammatory susceptibility by host cytokine induction. *Gut* 2018;67:97-107.

18. Touchefeu Y, Montassier E, Nieman K, et al. Systematic review: The role of the gut microbiota in chemotherapy- or radiation-induced gastrointestinal mucositis – current evidence and potential clinical applications. *Alimentary Pharmacology & Therapeutics* 2014;40:409-421.

19. Kim SB, Bozeman RG, Kaisani A, et al. Radiation promotes colorectal cancer initiation and progression by inducing senescence-associated inflammatory responses. *Oncogene* 2016;35:3365-3375.

20. Iida N, Dzutsev A, Stewart CA, et al. Commensal bacteria control cancer response to therapy by modulating the tumor microenvironment. *Science* 2013;342:967-70.

21. Gopalakrishnan V, Spencer CN, Nezi L, et al. Gut microbiome modulates response to anti–pd-1 immunotherapy in melanoma patients. *Science* 2018;359:97.

22. Matson V, Fessler J, Bao R, et al. The commensal microbiome is associated with anti–pd-1 efficacy in metastatic melanoma patients. *Science* 2018;359:104.

23. XXXX

24. XXXX

25.XXXX

26. XXXX

27. Mysara M, Njima M, Leys N, et al. From reads to operational taxonomic units: An ensemble processing pipeline for miseq amplicon sequencing data. *Gigascience* 2017;6:1-10.

28. Segata N, Izard J, Waldron L, et al. Metagenomic biomarker discovery and explanation. *Genome Biol* 2011;12:R60-R60.

29. Langille MGI, Zaneveld J, Caporaso JG, et al. Predictive functional profiling of microbial communities using 16s rrna marker gene sequences. *Nature biotechnology* 2013;31:814-821.

30. Parks DH, Tyson GW, Hugenholtz P, et al. Stamp: Statistical analysis of taxonomic and functional profiles. *Bioinformatics* 2014;30:3123-3124.

31. Field SB, Bewley DK. Effects of dose-rate on the radiation response of rat skin. *Int J Radiat Biol Relat Stud Phys Chem Med* 1974;26:259-67.

32. Inada T, Nishio H, Amino S, et al. High dose-rate dependence of early skin reaction in mouse. *Int J Radiat Biol Relat Stud Phys Chem Med* 1980;38:139-45.

33. Hendry JH, Moore JV, Hodgson BW, et al. The constant low oxygen concentration in all the target cells for mouse tail radionecrosis. *Radiat Res* 1982;92:172-81.

34. Favaudon V, Caplier L, Monceau V, et al. Ultrahigh dose-rate flash irradiation increases the differential response between normal and tumor tissue in mice. *Science translational medicine* 2014;6:245ra93.

35. Kim MM, Darafsheh A, Schuemann J, et al. Development of ultra-high dose rate (flash) particle therapy. *IEEE Transactions on Radiation and Plasma Medical Sciences* 2021:1-1.

36. Montay-Gruel P, Bouchet A, Jaccard M, et al. X-rays can trigger the flash effect: Ultra-high dose-rate synchrotron light source prevents normal brain injury after whole brain irradiation in mice. *Radiother Oncol* 2018.

37. ClinicalTrials.gov. Feasibility study of flash radiotherapy for the treatment of symptomatic bone metastases (fast-01). In: Editor, editor^editors. Book Feasibility study of flash radiotherapy for the treatment of symptomatic bone metastases (fast-01); 2020.

38. Diffenderfer ES, Verginadis II, Kim MM, et al. Design, implementation, and in vivo validation of a novel proton flash radiation therapy system. *Int J Radiat Oncol Biol Phys* 2020;106:440-448.

39. Zhang Q, Cascio E, Li C, et al. Flash investigations using protons: Design of delivery system, preclinical setup and confirmation of flash effect with protons in animal systems. *Radiat Res* 2020.

40. Wang Z, Wang Q, Wang X, et al. Gut microbial dysbiosis is associated with development and progression of radiation enteritis during pelvic radiotherapy. *J Cell Mol Med* 2019;23:3747-3756.

41. Li Y, Yan H, Zhang Y, et al. Alterations of the gut microbiome composition and lipid metabolic profile in radiation enteritis. *Front Cell Infect Microbiol* 2020;10:541178.

42. Manichanh C, Varela E, Martinez C, et al. The gut microbiota predispose to the pathophysiology of acute postradiotherapy diarrhea. *Am J Gastroenterol* 2008;103:1754-61.

43. Reis Ferreira M, Andreyev HJN, Mohammed K, et al. Microbiota- and radiotherapy-induced gastrointestinal side-effects (mars) study: A large pilot study of the microbiome in acute and late-radiation enteropathy. *Clin Cancer Res* 2019;25:6487-6500.

44. Li Y, Dong J, Xiao H, et al. Gut commensal derived-valeric acid protects against radiation injuries. *Gut Microbes* 2020;11:789-806.

45. Basile D, Di Nardo P, Corvaja C, et al. Mucosal injury during anti-cancer treatment: From pathobiology to bedside. *Cancers (Basel)* 2019;11.

46. Wang Q, Lin Y, Sheng X, et al. Arachidonic acid promotes intestinal regeneration by activating wnt signaling. *Stem Cell Reports* 2020;15:374-388.

47. Serbanescu MA, Mathena RP, Xu J, et al. General anesthesia alters the diversity and composition of the intestinal microbiota in mice. *Anesth Analg* 2019;129:e126-e129.

48. Levy K, Natarajan S, Wang J, et al. Abdominal flash irradiation reduces radiation-induced gastrointestinal toxicity for the treatment of ovarian cancer in mice. *Sci Rep* 2020;10:21600.

Figure Legends

Figure 1. Left: The mouse position in the cradle that was used for all the whole abdominal irradiations. Right: The mouse setup in the beam path, with the mouse aligned in the horizontal beam (goes from left to right) behind the energy monitor and collimator system.

Figure 2. Intestinal normal tissue response after conventional dose rate irradiation (CONV IR) vs. ultra-high dose rate irradiation (FLASH IR). Radiation dose response curve of small intestinal crypts for mice (C3H mice, female); A) aged 9-10 weeks (*n* = 6 for each group), B) aged 30-31 weeks (*n* = 4 for 0 Gy and 12.5 Gy FLASH IR, *n* = 6 for 5 Gy, *n* = 3 for the other groups). The individual data points were fitted with a sigmoidal dose response curve using the nonlinear regression analysis in GraphPad Prism. Error bars show standard error of the mean (SEM). * $p < 0.05$, ** $p < 0.01$. C) Representative H&E images of intestinal Swiss rolls from each treatment group. Scale bar = 200 μm.

Figure 3. Microbial profiling of fecal samples by 16S rRNA gene sequencing. A) Relative abundance bar plot of the detected operational taxonomic units (OTUs) for each sample. B) The α-diversity of microbiota as shown by the Inverse Simpson Index. C) Evenness of microbiota as shown by Simpson evenness index. D) Richness of microbiota as shown by Chao index. E) The β-diversity of microbiota as shown by PCoA plot. F) Taxonomic cladogram from LEfSe analysis showing differences in taxonomic clades with an LDA score > 3. *n* = 5 for conventional dose rate

irradiation (CONV IR), *n* = 6 for both ultra-high dose rate irradiation (FLASH IR) and control (CTRL). PCoA: Principle coordinate analysis. LEfSe: Linear discriminant analysis effect size. LDA: Linear discriminant analysis * $p < 0.05$, ** $p < 0.01$, *** $p < 0.001$.

Figure 4. Effect of radiation beam temporal pulse structure on crypt survival for 9–10-week-old (A-C) female C3H mice, following 11.2 Gy whole abdominal irradiation. As well as for 30–31-week-old (D-F) female C3H mice, following 12.5 Gy whole abdominal irradiation. Error bars show standard error of the mean (SEM). A) Effect of pulse number on crypt survival. *n* = 3 for 300 pulses and *n* = 4 for the remaining groups. B) Effect of pulse interval for a dual-pulse delivery on crypt survival. *n* = 3 for 30 sec and *n* = 4 for the remaining groups. C) Effect of total delivery time and average dose rate on crypt survival for both groups of mice combined. D) Effect of pulse number on crypt survival. *n* = 4 for 1, 100, and 300 pulses, *n* = 3 for 1250 pulses and *n* = 5 for the other groups. E) Effect of pulse interval for a dual-pulse delivery on crypt survival. *n* = 4 for 0.003 s and *n* = 5 for the other groups. F) Effect of total delivery time and average dose rate on crypt survival for both groups of mice combined.

Table 1. Temporal pulse structure characteristics and corresponding crypt survival for 11.2 Gy whole abdominal irradiation of mice aged 9-10 weeks

Number of pulses (n)	Dose-per-pulse (Gy)	Average dose rate (Gy/s)	Pulse dose rate (Gy/s)	Time interval between pulses (s)	Delivery time (s)	Crypt survival (%)	p-value, compared to single pulse delivery
1	11.2	3.3×10^{6}	3.3×10^{6}	-	3.4×10^{-6}	27.6 ± 4.0	-
2	5.60	3.4×10^{3}	1.6×10^{6}	3.3×10^{-3}	3.3×10^{-3}	14.9 ± 2.2	$p < 0.05$
2	5.60	1.1×10^{3}	1.6×10^{6}	0.010	0.010	13.2 ± 1.6	$p < 0.01$
2	5.60	280	1.6×10^{6}	0.040	0.040	6.9 ± 2.8	$p < 0.001$
2	5.60	3.7	1.6×10^{6}	3.0	3.0	8.1 ± 2.5	$p < 0.001$
2	5.60	0.37	1.6×10^{6}	30	30	6.4 ± 1.5	$p < 0.001$
5	2.24	280	6.6×10^{5}	0.010	0.040	13.8 ± 0.8	$p < 0.01$
30	0.370	39	1.1×10^{5}	0.010	0.29	11.5 ± 2.2	$p < 0.001$
100	0.112	11	3.2×10^{4}	0.010	1.0	6.7 ± 1.8	$p < 0.0001$
300	0.037	3.7	1.1×10^{4}	0.010	3.0	8.6 ± 1.3	$p < 0.001$

Table 2. Temporal pulse structure characteristics and corresponding crypt survival for 12.5 Gy whole abdominal irradiation of mice aged 30-31 weeks

Number of pulses (n)	Dose-per-pulse (Gy)	Average dose rate (Gy/s)	Pulse dose rate (Gy/s)	Time interval between pulses (s)	Delivery time (s)	Crypt survival (%)	p-value, compared to single pulse delivery
1	12.5	3.7×10^{6}	3.7×10^{6}	-	3.4×10^{-6}	11.0 ± 2.8	-
2	6.25	3.8×10^{3}	1.8×10^{6}	3.3×10^{-3}	3.3×10^{-3}	9.1 ±2.9	0.71
2	6.25	1.2×10^{3}	1.8×10^{6}	0.010	0.010	16.1 ± 5.8	0.92
2	6.25	310	1.8×10^{6}	0.040	0.040	15.3 ± 3.2	0.50
2	6.25	4.2	1.8×10^{6}	3.0	3.0	3.8 ± 0.2	$p < 0.05$
2	6.25	0.42	1.8×10^{6}	30	30	4.8 ± 0.9	0.11
5	2.50	310	7.4×10^{5}	0.010	0.040	7.8 ± 1.4	0.56
10	1.25	140	3.2×10^{5}	0.010	0.090	3.3 ± 1.0	$p < 0.05$
30	0.417	43	1.2×10^{5}	0.010	0.29	5.0 ± 1.8	0.11
100	0.125	13	3.7×10^{4}	0.010	1.0	6.1 ± 2.3	0.21
300	0.042	4.2	1.2×10^{4}	0.010	3.0	3.3 ± 1.1	$p < 0.05$
1250	0.010	0.25	2.9×10^{3}	0.040	50	1.3 ± 0.3	$p < 0.01$

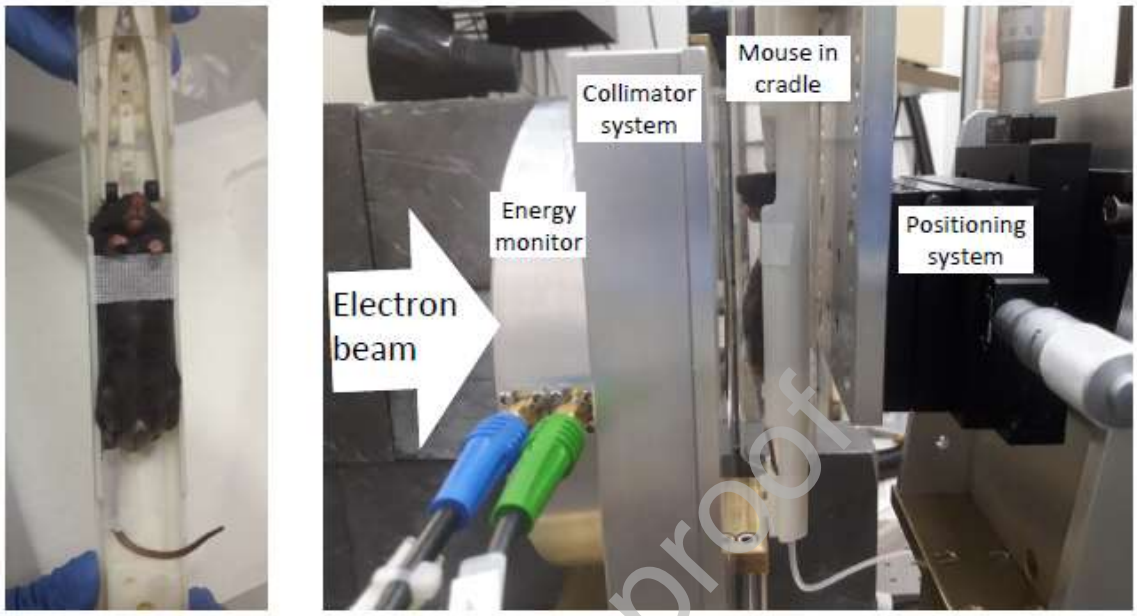

Fig. 1

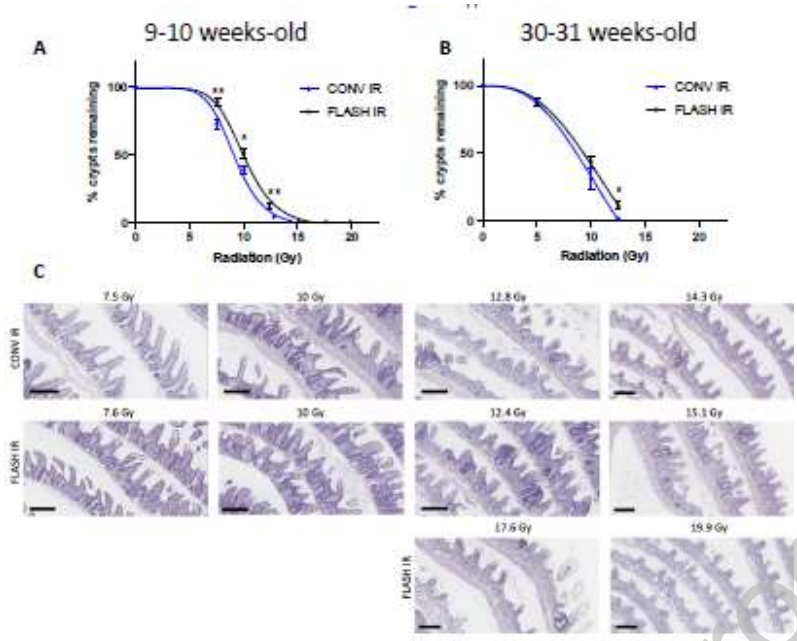

Fig. 2

Figure 3

Click here to access/download;Figure;Figure 3.pptx

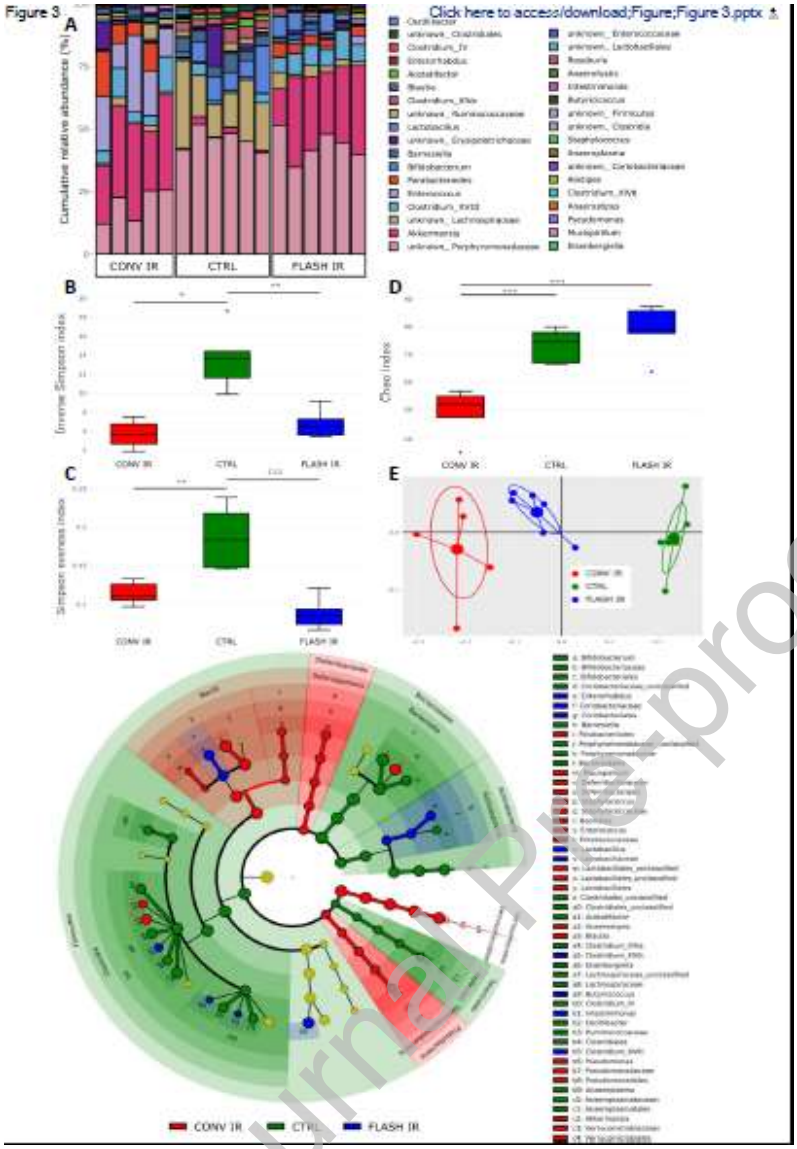

Fig. 3

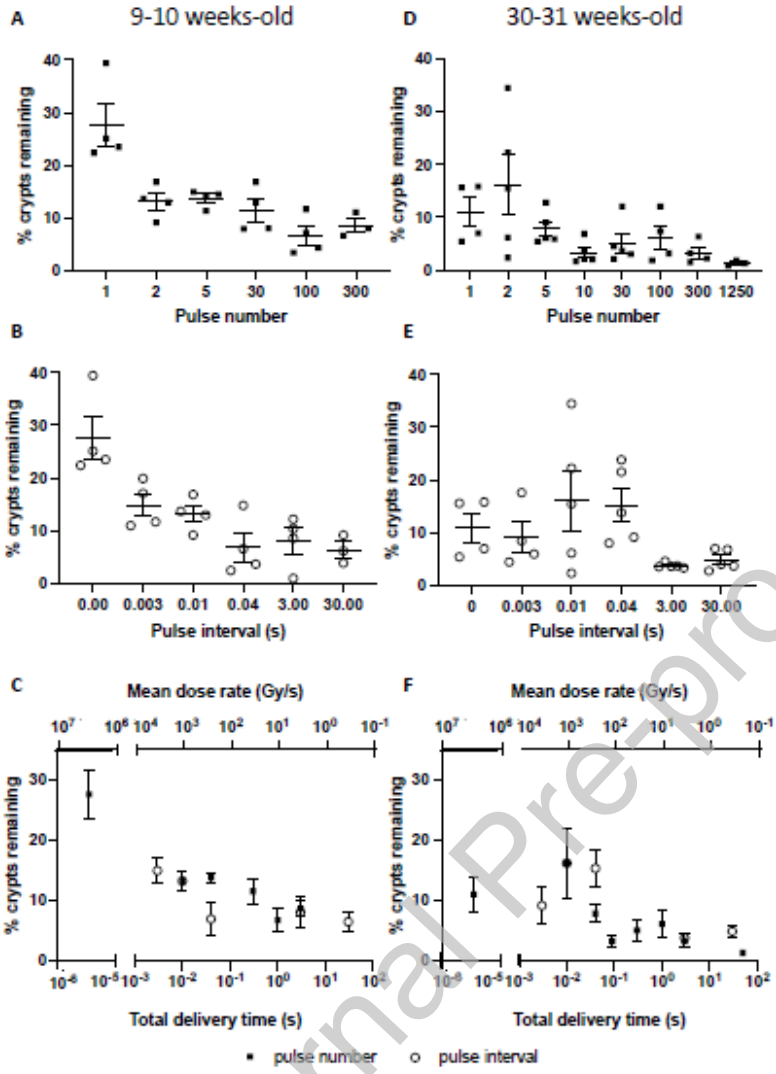

Fig. 4